3. Soot Optical Property Study

3.1 Introduction

Recent past studies of soot reaction processes in laminar premixed and nonpremixed flames generally have used the intrusive technique of thermophoretic sampling and analysis by transmission electron microscopy (TEM) to observe soot structure and obtain important fundamental information about soot particle properties, such as soot primary particle diameters, the rate of change of soot primary particle diameter as a function of time (or rate of soot surface growth or oxidation), the amount of soot particle reactive surface area per unit volume, the number of primary soot particles per unit volume, and the rate of formation of primary soot particles (or the rate of soot primary particle nucleation) [14-16,42-44]. Given the soot volume per unit volume of the flame (or the soot volume fraction), all these properties are readily found from a measurement of the soot primary particle diameter (which usually is nearly a constant for each location within a laminar flame) [14]. This approach is not possible within freely-propagating flames, however, because soot properties at given positions in such flames vary relatively rapidly as a function of time in the soot formation and oxidation regions compared to the relatively lengthy sampling times needed to accumulate adequate soot samples and to minimize effects of soot collected on the sampling grid as it moves to and from the sampling position through other portions of the flame. Thus, nonintrusive optical methods must be used to find the soot primary particle diameters needed to define the soot surface reaction properties mentioned earlier. Unfortunately, approximate nonintrusive methods used during early studies of soot reaction properties in flames, found from laser scattering and absorption measurements analyzed assuming either Rayleigh scattering or Mie scattering from polydisperse effective soot particles having the same mass of soot as individual soot aggregates, have not been found to be an effective way to estimate the soot surface reaction area per unit volume [45]. Thus, alternative nonintrusive optical methods of finding these properties must be sought, which was the objective of this phase of the investigation. The alternative method used here involves use of the Rayleigh-Debye-Gans-Polydisperse-Fractal-Aggregate (RDG-PFA) scattering approximation for soot aggregates in flames. Thus, the development of this method will be discussed next before describing its evaluation as a means of nonintrusively measuring soot primary particle diameters in soot-containing flames.

Past studies have made significant progress toward resolving the extinction and scattering properties of soot, see Charalampopoulos [46], Faeth and Koylu [47], Julien and Botet [48], Tien and Lee [49], and Viskanta and Mengüc [50]. This work has shown that soot consists of nearly monodisperse spherical primary particles collected into mass fractal aggregates, that primary soot particle diameters and the number of primary particles per aggregate vary widely whereas soot fractal properties are relatively universal, that soot optical properties can be approximated

by Rayleigh-Debye-Gans (RDG) scattering from polydisperse mass fractal aggregates (called RDG-PFA theory) at visible wavelengths and that accurate estimates of soot optical properties are mainly limited by uncertainties about soot refractive index properties. Earlier work in this laboratory due to Krishnan et al. [51] sought to improve understanding of soot refractive index properties in the visible by completing *in situ* measurements of soot coefficients and interpreting these results using RDG-PFA theory. The objective of the present investigation was to extend this research, concentrating on additional measurements and analysis of soot extinction and scattering properties in the near ultraviolet, visible and infrared wavelength ranges (wavelengths of 250-5200 nm), in an effort to establish a nonintrusive way to measure soot primary particle diameters.

Earlier studies of soot extinction and scattering properties are reviewed by Wu et al. [52]; therefore, the following discussion will be limited to the findings of the companion study of Krishnan et al. [51]. Krishnan et al. [51] carried out *in situ* measurements of the optical properties of soot at wavelengths of 351.2-800.0 nm, considering soot in the overfire region of large buoyant turbulent diffusion flames burning in still air at standard temperature and pressure and at long characteristic flame residence times where soot properties are independent of position and characteristic flame residence time for a particular fuel [53], considering soot in flames fueled with a variety of gaseous and liquid hydrocarbons (acetylene, ethylene, propylene, butadiene, benzene, cyclohexane, toluene and n-heptane). Extinction and scattering were interpreted to find soot optical properties using RDG-PFA theory after establishing that this theory was effective over the test range. Effects of fuel type on soot optical properties were comparable to experimental uncertainties. Dimensionless extinction coefficients were relatively independent of wavelength for wavelengths of 400-800 nm and yielded a mean value of 8.4 in good agreement with earlier measurements of Dobbins et al. [54], Choi et al. [55], Mulholland and Choi [56] and Zhou et al. [57] who considered similar overfire soot populations. Measurements of the refractive index function for absorption, E(m), were in good agreement with earlier *ex situ* reflectrometry measurements of Dalzell and Sarofim [58] and Stagg and Charalampopoulos [59]. On the other hand, measured values of the refractive index function for scattering, F(m), only agreed with these earlier measurements for wavelengths of 400-550 nm but otherwise increased with increasing wavelength more rapidly than the rest. These measurements also showed that refractive index function increased rapidly with increasing wavelength in the visible, yielding large levels of scattering as the infrared wavelength range was approached. This behavior raises concerns about approximation of modest refractive index values in the infrared that are required by RDG-PFA theory [54,60,61]; as well as concerns about the common assumption that scattering from soot in the infrared can be neglected when estimating flame radiation properties [49,50]. Finally, these results showed that soot refractive index properties do not approach the resonance condition in the near ultraviolet that is observed for graphite, see Chang and Charalampopoulos [62]; instead, refractive indices declined

continuously with decreasing wavelength as the near ultraviolet was approached, similar to the findings of Vaglieco et al. [63] for amorphous carbon and soot.

The present study sought to extend the measurements of Krishnan et al. [51] into both the infrared and the near ultraviolet to help resolve concerns about soot optical properties in these spectral regions. Other issues that were considered included evaluating scattering predictions in the visible and infrared based on RDG-PFA theory, developing information about depolarization ratios in the visible that is needed to properly close scattering predictions based on RDG-PFA theory, and exploiting RDG-PFA theory to evaluate variation of soot refractive index properties with full type and wavelength. The following description of the study is brief; more details can be found in Krishnan et al. [64].

3.2 Experimental Methods

The experimental arrangement was the same as Krishnan et al. [51]. A sketch of the apparatus appears in Fig. 10. The apparatus consisted of either a water-cooled gas-fueled burner having a diameter of 50 mm, or uncooled liquid-fueled burners having diameters of 51 and 102 mm, all injecting fuel gases vertically upward. The burners were located within an enclosure having a hood with a 152 mm diameter vertical exhaust duct at the top. Measurements were made at the exit of the exhaust duct where flow properties were nearly uniform. All operating conditions involved buoyant turbulent diffusion flames in still air within the long residence time regime where soot in the fuel-lean (overfire) region is independent of position and characteristic flame residence time [53].

Many of the properties of the present overfire soot were available from earlier measurements by [51-53,65-67], as follows: density, composition, volume fractions (gravimetrically), primary particle diameters, aggregate size properties ($\overline{N}$,N_g,σ_g), aggregate fractal dimensions, scattering and extinction properties in the visible, and refractive index properties in the visible. Present measurements emphasized extinction within the wavelength range of 250-5200 nm. The wavelengths that were considered and the light sources that were used are as follows: 351.2, 457.9, 488.0 and 514.5 nm using an argon-ion laser (4W, Coherent Innova 90-4); 632.8 nm using a He-Ne laser (28 mW, Jodon HN10G1R); 248.0, 303.0, 405.0, 4360, 546.0 and 578.0 nm using a mercury lamp (100W, Oriel 6281); 600.0, 800.0, 1100.0, 1550.0 and 2017.0 nm using a Quartz-Tungsten Halogen (QTH) lamp (100W, Oriel 6333); and 3980.0 and 5205.0 nm using an IR emitter source (Oriel 6363). Two detectors were used, as follows: 351.2-800.0 nm using a silicon detector (Newport 818-UV), and 248.0-303.0 nm and 1100.0-5205.0 nm using a pyrodetector (Oriel 70128). Interference filters having 10 nm bandwidths were used for wavelengths up to 1550.0 nm; interference filters having bandwidths of 90-160 nm were used for wavelengths larger than 1500.0 nm. The optical arrangement was

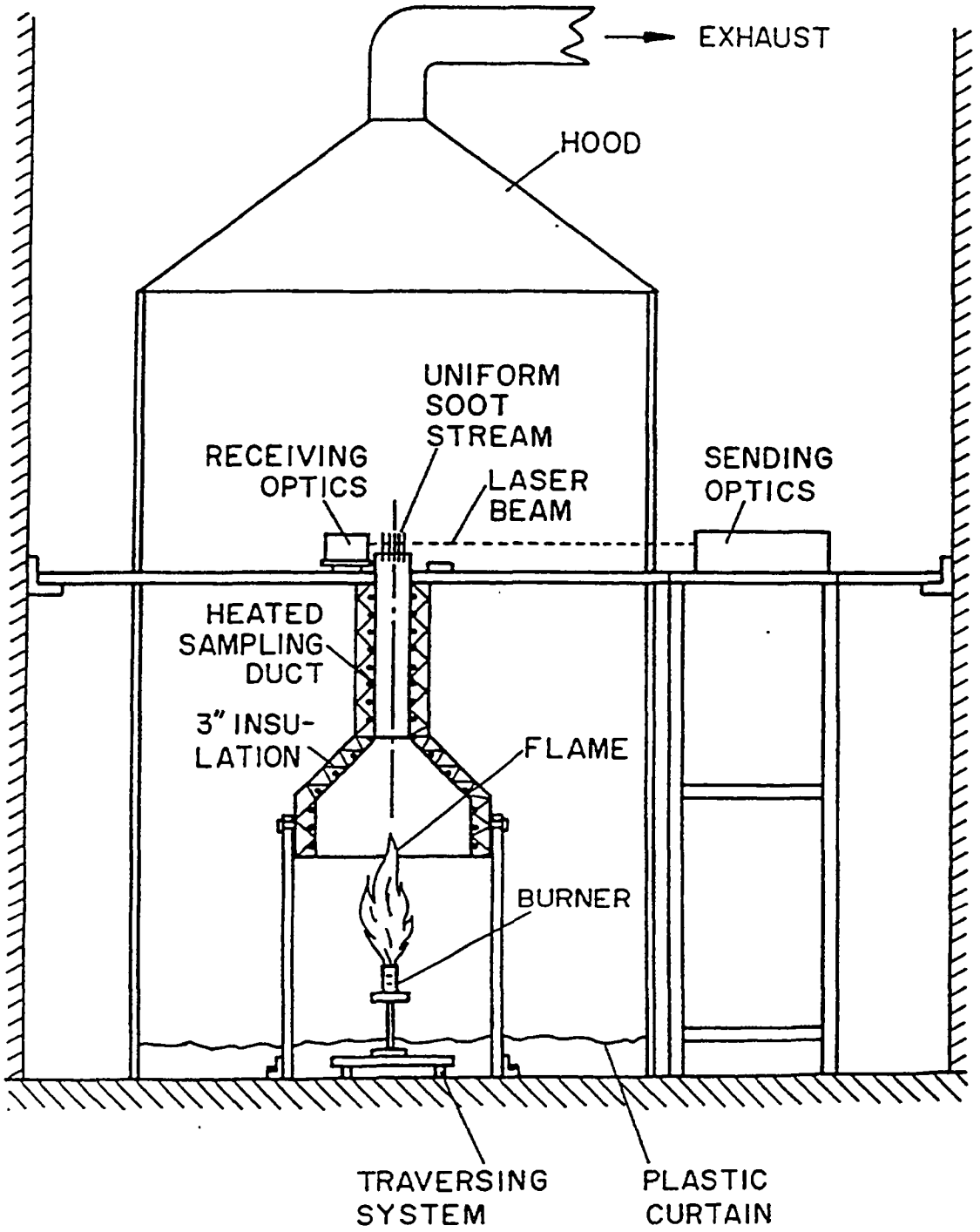

Fig. 10. Sketch of the experimental apparatus for light scattering and extinction measurements.

designed following Manickavasagam and Mengüc [68] to reduce contributions from forward scattering to extinction measurements to less than 1 percent. Calcium fluoride lenses were used for spatial filtering and collimating the incident light due to the large range of wavelengths considered. The light was modulated by a chopper (SR 540) before passing through the soot-containing exhaust flow. The output of the detector was passed through lock-in amplifiers prior to sampling and storage using a laboratory computer. Sampling was done at 2 kHz for a time period of 60s, averaging results for three sampling periods at each wavelength. Experimental uncertainties (95% confidence) of the extinction measurements are estimated to be less than 5%. Experimental uncertainties of the other measurements will be presented when they are discussed.

The test conditions were the same as Krishnan et al. [51]. A brief summary of the fuels considered, and the corresponding structure properties of the overfire soot, is presented in Table 2. This range of fuels provides evaluation of soot optical properties for H/C atomic ratios of 1.00-2.28.

The test conditions were the same as Krishnan et al. (2000). A brief summary of the fuels considered, and the corresponding structure properties of the overfire soot, is presented in Table 1. This range of fuels provides evaluation of soot optical properties for H/C atomic ratios of 1.00-2.28.

3.3 Theoretical Methods

Analysis of the extinction and scattering measurements to find soot optical properties was based on RDG-PFA theory. Portions of this theory used during the present investigation are briefly summarized in the following, see Julien and Botet [48], Dobbins and Megaridis [60], Koylu and Faeth [65] and references cited therein for more details.

The main assumptions of RDG-PFA theory are as follows: individual primary particles are Rayleigh scattering objects, aggregates satisfy the RDG scattering approximations, primary particles are spherical and have constant diameters, primary particles just touch one another, the number of primary particles per aggregate satisfies a log-normal probability distribution function, and aggregates are mass fractal objects that satisfy the following relationship (Julien and Botet, [48]:

$$N = k_f (R_g / d_p)^{D_f} \tag{6}$$

These approximations have proven to be satisfactory during past evaluations of RDG-PFA theory for a variety of conditions, including soot populations similar to the present study, see

Krishnan [51], Wu et al. [52] and Koylu and Faeth [65,66,69]; nevertheless, the theory was still evaluated during the present investigation before applying it to find soot optical and scattering properties.

The following formulation will be in terms of volumetric optical cross sections; these can be converted to optical cross sections, as follows:

$$\overline{C}_j^a = \overline{NQ}_j^a/n_p; \quad j=vv,hh,s,a,e \tag{7}$$

The volumetric extinction cross section is simply the sum of the volumetric absorption and total scattering cross sections,

$$\overline{Q}_e^a = \overline{Q}_a^a + \overline{Q}_s^a = (1+\rho_{sa})\overline{Q}_a^a \tag{8}$$

where the last expression introduces the total scattering/absorption cross section ratio:

$$\rho_{sa} = \overline{Q}_s^a / \overline{Q}_a^a \tag{9}$$

Based on RDG-PFA theory, ρ_{sa} can be computed given the structure and refractive index properties of the soot population, when effects of depolarization are small, as follows:

$$\rho_{sa} = 2x_p^3 F(m)\,\overline{N^2 g}/(3E(m)\overline{N}) \tag{10}$$

The specific expression for the aggregate total scattering factor, $g(kR_g,D_f)$, and the method of computing $\overline{N^2 g}$ from known aggregate structure properties, are described by Koylu and Faeth [65].

In order to complete predictions of soot extinction and scattering properties using RDG-PFA theory, measurements of soot volume fractions (gravimetrically) and primary particle diameters (by thermophoretic sampling and transmission electron microscopy, TEM) were used to compute primary particle density, as follows:

$$n_p = 6f_v/(\pi d_p^3) \tag{11}$$

Present extinction and scattering measurements in the visible yield $\overline{Q}_e^a$ and $\overline{Q}_s^a$ directly, so that $\overline{Q}_a^a$ can be found from Eq. (8) and ρ_{sa} from Eq. (9). Then the refractive index functions can be computed from the RDG-PFA formulation, as follows:

$$E(m) = k^2 \overline{Q}_a^a / (4\pi x_p^3 n_p) \quad (12)$$

$$F(m) = k^2 (qd_p)^{D_f} \overline{Q}_{vv}^a (qd_p) / (k_f x_p^6 n_p) \quad (13)$$

where qd_p must be large enough so that scattering is in the large-angle (power-law) regime where Eq. (13) is appropriate. This last requirement was readily satisfied because power-law scattering dominated the scattering properties of the present large soot aggregates, see Wu et al. [52]. The fractal properties needed to apply Eq. (13) also were known for the present soot populations, see Table 2. Finally, combining Eqs. (11) and (12) yields a useful expression for $\overline{Q}_a^a$, as follows:

Table 2. Summary of soot structure properties[a]

Fuel	d_p (nm)	$\overline{N}$	N_g	σ_g	$D_f(\sigma_D)^b$
Gas-fueled flames:					
Acetylene	47	417	214	3.3	1.79 (0.01)
Butadiene	42[c]	---	---	---	1.79 (0.03)
Propylene	41	460	227	3.0	1.79 (0.02)
Ethylene	32	467	290	2.7	1.80 (0.01)
Liquid-fueled flames:					
Toluene	51	526	252	3.2	1.79 (0.07)
Benzene	50	552	261	3.5	1.77 (0.05)
Cyclohexane	37[c]	---	---	---	1.80 (0.06)
n-Heptane	35	260	173	2.4	1.79 (0.06)

[a]Soot in the overfire region of buoyant turbulent diffusion flames burning in still air in the long residence time regime with ambient pressures and temperatures of 99 ± 0.5 kPa and 298 ± 3 K, respectively. Soot density of 1880 kg/m^3 from Wu et al. [52]; $k_f = 8.5$ with a standard deviation of 0.5 from Koylu et al. [67]. Values of d_p, $\overline{N}$, n_g and σ_g from Koylu and Faeth [53] and Koylu and Faeth [65] except when noted otherwise. The list is in order of progressively decreasing primary particle diameter for gas- and liquid-fueled flames, respectively.

$$\overline{Q}_a^a = 6\pi E(m) f_v / \lambda \tag{14}$$

Large soot aggregates exhibit effects of depolarization which influence $\overline{Q}_{hh}^a$ and thus estimates of $\overline{Q}_s^a$ and ρ_{sa}. Unfortunately, effects of depolarization cannot be predicted using RDG-PFA theory and must be handled empirically instead. This was done as suggested by Koylu and Faeth [65] by defining a depolarization ratio, ρ_v, and using it analogous to Rayleigh scattering theory, see Rudder and Bach [70]. Thus, values of $\overline{Q}_{hh}^a(\theta)$ were found, as follows:

$$\overline{Q}_{hh}^a(\theta) = \left[(1-\rho_v)\cos^2\theta + \rho_v\right]\overline{Q}_{vv}^a(\theta) \tag{15}$$

It follows immediately from Eq. (15) that [65]

$$\rho_v = \overline{Q}_{hh}^a(90^\circ)/\overline{Q}_{vv}^a(90^\circ) \tag{16}$$

so that ρ_v could be obtained directly from present measurements in the visible.

The formulation of Eqs. (6)-(16) was used in several ways during the present investigation. First of all, normalized parameters, e.g., $\overline{Q}_{vv}^a(\theta)/\overline{Q}_{vv}^a(90^\circ)$ and $\overline{Q}_{hh}^a(\theta)/\overline{Q}_{vv}^a(90^\circ)$, yield scattering patterns that are independent of refractive index properties from Eqs. (12)-(16) and can be used to evaluate RDG-PFA predictions and find values of ρ_v from the measurements. In addition, all quantities on the right hand sides of Eqs. (12) and (13) were known in the visible so that these equations could be used to find E(m) and F(m) in the visible as discussed by Krishnan et al. [51]. Effects of depolarization on predictions of total scattering cross sections were small so that Eq. (10) could be used to predict ρ_{sa} in the visible, given values of E(m) and F(m), providing a means of testing combined effects of RDG-PFA predictions and refractive index property measurements. Then, Eq. (10) was used to estimate ρ_{sa} in the infrared (after finding a correlation for F(m)/E(m) in the infrared to be discussed later) so that E(m) could be found from present measurements of $\overline{Q}_e^a$ using Eqs. (8) and (14). Finally, Eq. (10) in conjunction with values of E(m) and F(m) developed from the measurements, were used to estimate the potential importance of scattering from soot on the properties of flame radiation.

3.4 Results and Discussion

Scattering Patterns. Typical examples of measured and predicted scattering patterns (ethylene soot at wavelengths of 351.2-632.8 nm) appear in Fig. 11, see Krishnan et al. [51] Wu et al. [52] and Koylu and Faeth [65] for other examples. Experimental uncertainties (95% confidence) of the normalized scattering properties illustrated in Fig. 11, are estimated to be smaller than 10%, except for the hh component near 90 deg, where small values of this ratio

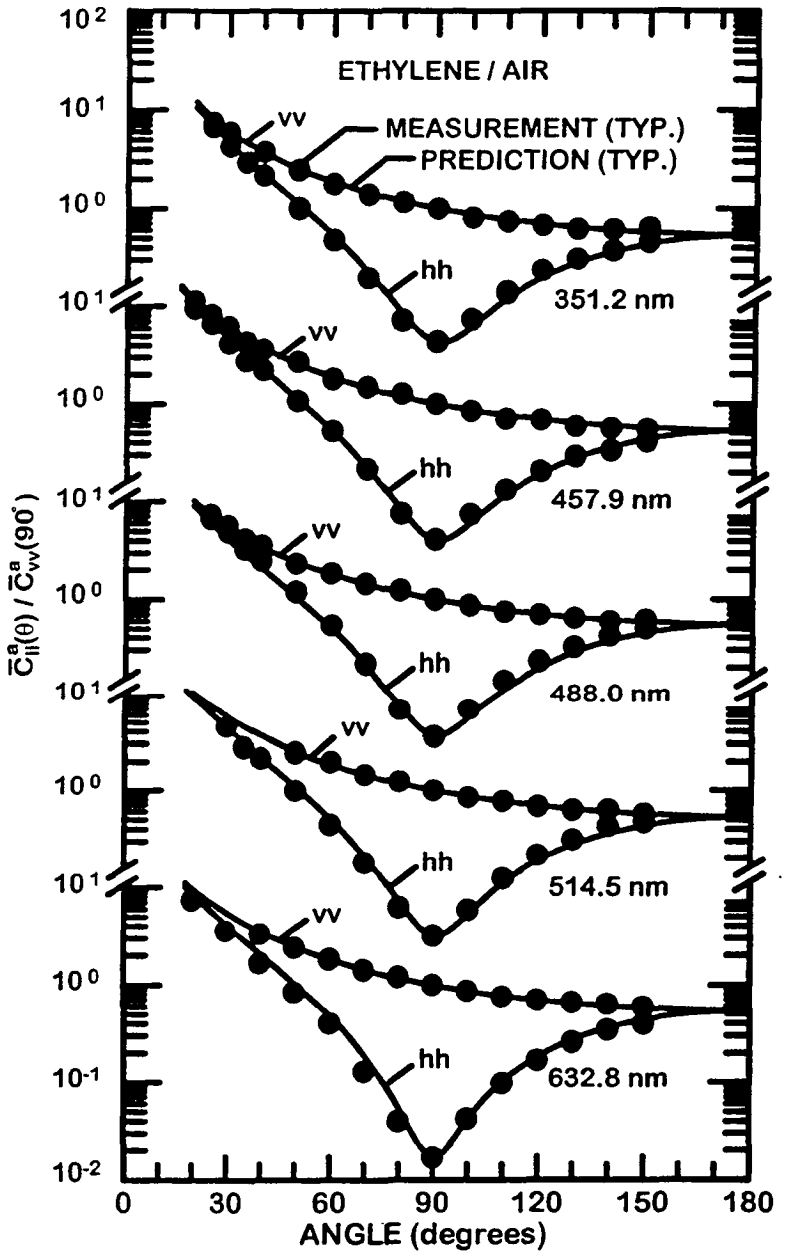

Fig. 11. Measured and predicted scattering patterns of soot in ethylene/air flames at wavelengths in the visible (351.2-632.8 nm). From Krishnan et al. [64].

make uncertainties somewhat larger. The agreement between measurements and predictions is excellent with discrepancies smaller than experimental uncertainties. In particular, there is no deterioration of predictions at small wavelengths where relatively large values of x_p create concerns about the validity of RDG-PFA theory [51]. Similarly, there is no deterioration of performance at large wavelengths where progressively increasing values of the real and imaginary parts of the refractive indices of soot with increased wavelength also cause concerns about the validity of RDG-PFA theory [51]. Similar performance was achieved at other conditions implying acceptable use of RDG-PFA theory for soot at values of x_p as large as 0.46. This general behavior, involving variations of both wavelength and refractive indices to justify the use of RDG-PFA theory, agrees with the detailed computational evaluations of Farias et al. [71] concerning the range of validity of RDG-PFA theory.

Depolarization Ratios. A limitation of RDG-PFA theory is that it provides no estimates of depolarization ratios that are needed to compute $\overline{Q}^a_{hh}(\theta)$ from Eq. (15). Thus, measurements of ρ_v were completed so that computations to find ρ_{sa} in the near infrared could be undertaken. This work involved exploiting the available data base of scattering patterns in the literature, using Eq. (16) to find ρ_v. Available measurements of ρ_v are plotted as a function of x_p in Fig. 12. Measurements illustrated in the plot include results from Krishnan et al. [51], Wu et al. [52], Koylu and Faeth [65,69] and the present investigation. Experimental uncertainties (95% confidence) of these determinations are somewhat larger than those of $\overline{Q}^a_{vv}(\theta)/\overline{Q}^a_{vv}(90°)$ due to the small magnitude of ρ_v but are still estimated to be smaller than 20%. Results for soot in the overfire region of buoyant turbulent diffusion flames in the long residence time regimes, due Krishnan et al. [51], Wu et al. [52], Koylu and Faeth [65] and the present investigation, are relatively independent of fuel type and are in reasonable agreement with each other, yielding the following correlation for ρ_v:

$$\rho_v = 0.14 x_p \tag{17}$$

which also is shown on the plot. The standard error of the power of x_p in Eq. (17) is 0.1, the standard error of the coefficient is 0.03, and the correlation coefficient of the fit is 0.83, which is reasonably good. This is not surprising because relationships between the size of scattering objects and depolarization ratio have been recognized for some time [70,72], including recent observations of diStasio [73] of a relationship between primary soot particle diameter and depolarization ratio analogous to the present findings. In contrast, the measurements for underfire soot in laminar diffusion flames due to Koylu and Faeth [69] are consistently smaller (by roughly 35%) than results for the overfire soot, although the variation of ρ_v with x_p is similar. This behavior suggests that the coefficient of Eq. (17) may be a function of aggregate size because the underfire soot involved $\overline{N}$ in the range 30-80 whereas the overfire soot involved $\overline{N}$

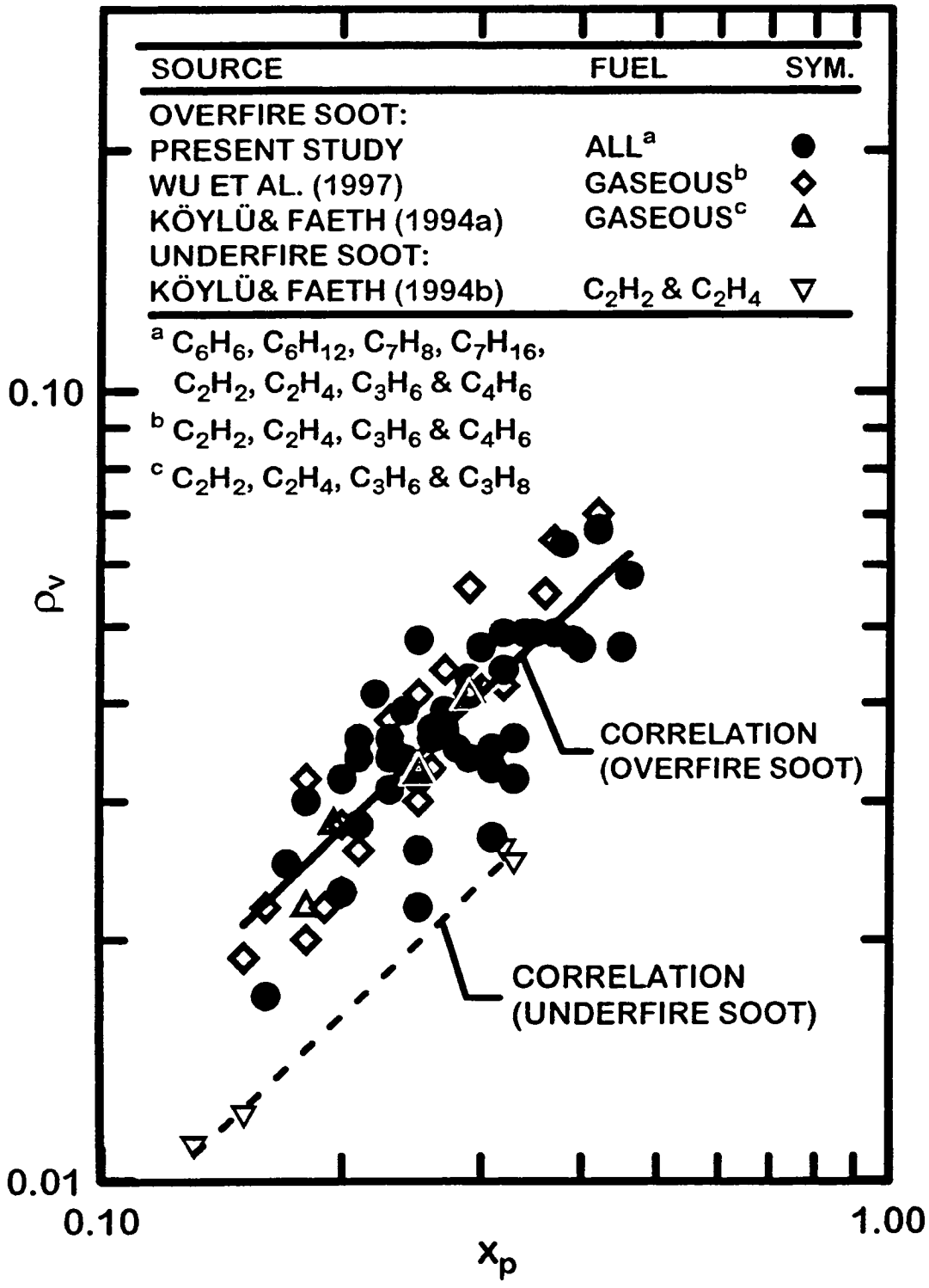

Fig. 12. Measurements of depolarization ratios of various fuels as a function of primary particle size parameter in the visible (351.2-632.8 nm). Measurements of Wu et al. [52], Koylu and Faeth [65,69] and Krishnan et al. [64]. From Krishnan et al. [64].

in the range 260-552 (see Table 2 for the latter). Finally, the values of ρ_v for soot aggregates illustrated in Fig. 12 are roughly an order of magnitude larger than typical values of ρ_v for Rayleigh scattering from gases, see Rudder and Bach [70]; this behavior is consistent with the much smaller values of x_p for gases than for soot.

Refractive Index Functions. Values of F(m)/E(m) and E(m) are needed to find spectral radiation properties and nonintrusive measurements of soot volume fractions, see Eqs. (10), (12), (13), and (14). Values of F(m)/E(m) for wavelengths of 350-9000 nm are illustrated in Fig. 13. Results shown include the *ex situ* reflectometry measurements of Dalzell and Sarofim [58], Stagg and Charalampopoulos [59], and Felske et al. [74] and the *in situ* absorption and scattering measurements in the visible of Wu et al. [52] and Krishnan et al. [51]. The measurements of Dalzell and Sarofim [58] are averages of their results for acetylene- and propane-fueled flames. The measurements of Wu et al. [52] have been adjusted to correct an error in their gravimetric determinations of soot volume fractions by matching their dimensionless extinction coefficients to the present measurements at 514.5 nm as discussed by Krishnan et al. [51]. Other measurements due to Chang and Charalampopoulos [62], Vaglieco et al. [63], Batten [75], Lee and Tien [76], and have not been included on the plot due to concerns about either experimental methods or about methods used to interpret measurements as discussed by Krishnan et al. [51]. Finally, two empirical correlations of the measurements are illustrated on the plot: one for the measurements of Krishnan et al. [51] for wavelengths of 350-650 nm and one for all the measurements for wavelengths 350-6000 nm.

The measurements of F(m)/E(m) illustrated in Fig. 13 involve various fuels, sources and methods and are in remarkably good agreement. Exceptions involve the early *ex situ* reflectometry measurements of Dalzell and Sarofim [58]; they provide low estimates in the visible which may be due to the fact that corrections were not made for effects of surface voids on scattering properties which are important in the visible [74]; and they provide high estimates in the far infrared at wavelengths larger than 6000 nm where small scattering levels and corresponding poor signal-to-noise ratios may be a factor. The relatively good agreement among the measurements at other conditions is no doubt promoted by the fact that F(m)/E(m) involves ratios of scattering to absorption cross sections which tend to normalize the measurements and reduce errors compared to measurements of absorption and scattering alone and the fact that corrections of the *ex situ* results for effects of surface roughness should be relatively small in the infrared [74]. Nevertheless, in view of past criticism of the *ex situ* measurements of Dalzell and Sarofim [58] and Felske et al. [74] their measured velocity values of F(m)/E(m) in the infrared clearly merit reconsideration.

The absorption and scattering measurements of Krishnan et al. [51] and the corrected absorption and scattering measurements of Wu et al. [52], both in the visible, provide complete

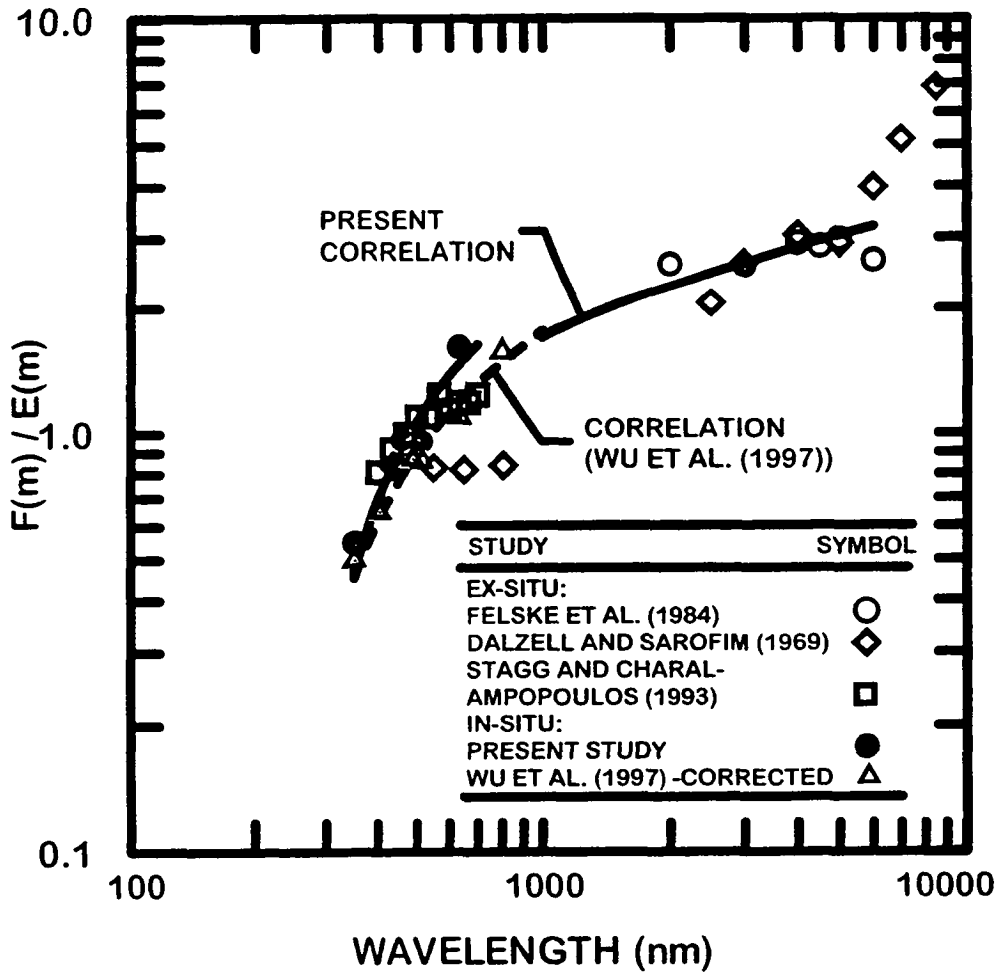

Fig. 13. Measurements of the refractive index function ratios F(m)/E(m) of various fuels as a function of wavelength for wavelengths of 250-9000 nm. *Ex situ* measurements of Dalzell and Sarofim [58] and Stagg and Charalampopoulos [59]; *in situ* measurements of Krishnan et al. [51] and Wu et al. [52]. From Krishnan et al. [64].

information needed to find ρ_{sa} and E(m) in the visible using Eqs. (12) and (13). In addition, ρ_{sa} becomes small at the largest wavelengths considered during the present investigation so that present measured values of $\overline{Q}_e^a \approx \overline{Q}_a^a$ and E(m) can be found directly from Eq. (12). At intermediate wavelengths, however, RDG-PFA theory was used to estimate values of ρ_{sa} so that $\overline{Q}_a^a$ could be found from the extinction measurements and then E(m) from Eq. (12). These estimates of ρ_{sa} were obtained using the correlation of F(m)/E(m) illustrated in Fig. 13, the known structure properties of the present soot and the RDG-PFA results of Eq. (10). Another set of *in situ* measurements of E(m) was obtained from the earlier extinction measurements of Koylu and Faeth [66]: this was done by matching values of E(m) from Krishnan et al. [51] with these results at 514.5 nm and then using present measurements and estimates of ρ_{sa} in the visible and infrared to find E(m) from Eq. (12). Finally, the *ex situ* reflectometry measurements of Dalzell and Sarofim [58], Stagg and Charalampopoulos [59] and Felske et al. [74] directly provide values of E(m).

The various determinations of E(m) for wavelengths of 350-9000 nm are illustrated in Fig. 14. The various *in situ* measurements of E(m) agree within experimental uncertainties over the entire wavelength range of the measurements which is encouraging. The *in situ* and *ex situ* measurements of E(m) in the visible agree within experimental uncertainties, with the somewhat smaller values of E(m) for the *ex situ* measurements attributed to uncorrected effects of surface voidage, at least for the measurements of Dalzell and Sarofim [58]. More disconcerting, however, are the unusually small values of E(m) found from the *ex situ* reflectometry measurements of Dalzell and Sarofim [58] and Felske et al. [74] in the infrared at wavelengths of 2000-9000 nm. In particular, it is difficult to see how trends of constant or progressively decreasing values of E(m) with increasing wavelength could yield the slightly increasing values of K_e with increasing wavelength in the infrared seen for RDG scattering objects [64]. In contrast, present values of E(m) expressly yield the trends of K_e illustrated in Ref. 64 due to the method used to find E(m). Nevertheless, resolving the differences between the *in situ* and *ex situ* determinations of E(m) seen in Fig. 14 merits priority because these differences clearly can have a large impact on the radiative properties of soot-containing flames which are dominated by continuum radiation from soot in the infrared.

3.5 Conclusions

The extinction and scattering properties of soot were studied using *in situ* methods at wavelengths of 250-5200 nm. Test conditions were limited to soot in the fuel-lean (overfire) region of buoyant turbulent diffusion flames in the long residence time regime where soot properties are independent of position and characteristic flame residence time. Flames burning in still air and fueled with eight liquid and gas hydrocarbon fuels were considered to provide atomic

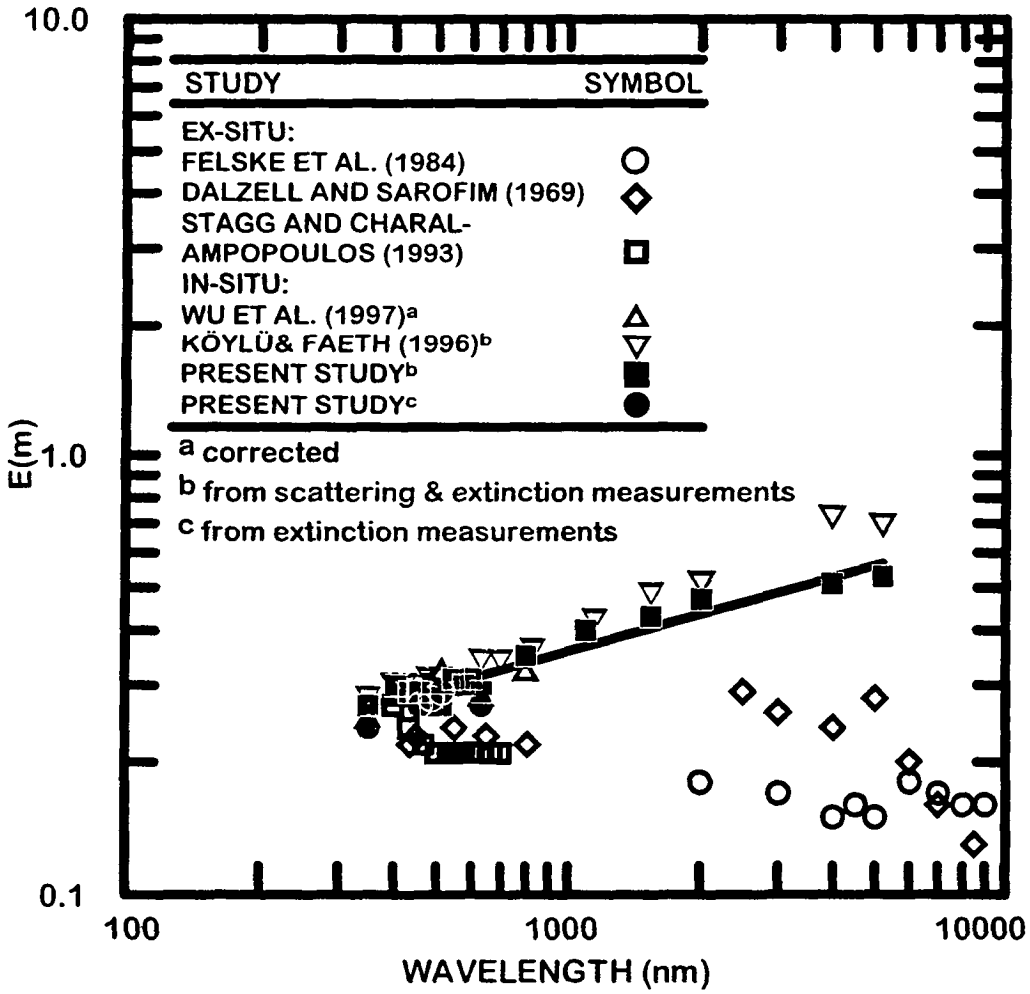

Fig. 14. Measurements of the refractive index function for absorption, E(m), of various fuels as a function of wavelength for wavelengths of 250-9000 nm. *Ex situ* measurements of Dalzell and Sarofim [58], Stagg and Charalampopoulos [59] and Felske et al. [74]; *in situ* results of Krishnan et al. [51], Wu et al. [52], Koylu and Faeth [69] and Krishnan et al. [64]. From Krishnan et al. [64].

H/C ratios in the range 1.00-2.28. RDG-PFA theory was used to interpret the measurements based on successful evaluation of this theory over the test range (values of x_p up to 0.46). The major conclusions of the study are as follows:

1. Present *in situ* measurements of the ratios of the scattering/absorption refractive index function, F(m)/E(m), were independent of fuel type and were in good agreement with earlier *ex situ* measurements in the literature. Present *in situ* measurements of the refractive index function for absorption, E(m), were also independent of fuel type and were in good agreement with earlier *in situ* measurements but were somewhat larger than earlier *ex situ* reflectometry measurements in the infrared.

2. Measured depolarization ratios yielded a somewhat scattered but simple correlation in terms of the primary particle size parameter alone in terms of the primary particle size parameter alone as suggested in recent work of diStasio [73]. Given a correlation along these lines, the methodology needed to compute scattering properties according to RDG-PFA theory would be completed and a simple nonintrusive diagnostic would be feasible. Effects of aggregate size on this correlation were observed, however, and merit further study in the future before these methods can be reliably used.

Other conclusions of this phase of the investigation are discussed in Krishnan et al. [64]. Extending these conclusions to other types of soot should be approached with caution. In particular, the present soot has been exposed to oxidation in flame environments and involves relatively large soot aggregates due to large characteristic flame residence times; thus, such soot may not be representative of unoxidized and weakly aggregated soot typical of fuel-rich soot growth regions.

References

1. Bockhorn, H., Fetting, F., Wannemacher, G. and Wentz, H. W., *Proc. Combust. Inst.* 19:1413-1420 (1982).

2. Bockhorn, H., Fetting, F., Heddrich, A. and Wannemacher, G., *Proc. Combust. Inst.* 20:979-988 (1984).

3. Bockhorn, H., Fetting, F. and Heddrich, A., *Proc. Combust. Inst.* 21:1001-1012 (1996).

4. Wieschnowsky, V., Bockhorn, H. and Fetting, F., *Proc. Combust. Inst.* 22:343-352 (1988).

5. Harris, S.J. and Weiner, A.M., *Combust. Sci. Tech.* 31:155-167 (1983).

6. Harris, S.J. and Weiner, A.M., *Combust. Sci. Tech.* 32:267-275(1983).

7. Harris, S.J. and Weiner, A.M., *Combust. Sci. Tech.* 38:75-87 (1984).

8. Ramer, E.R., Merklin, J.F., Sorensen, C.M. and Taylor, T.W., *Combust. Sci. Tech.* 48:241-255 (1986).

9. Mätzing, H. and Wagner, H. Gg., *Proc. Combust. Inst.* 21:1047-1055 (1986).

10. Böhm, H., Hesse, D., Jander, H., Lüers, B., Pietscher, J., Wagner, H.Gg. and Weiss, M., *Proc. Combust. Inst.* 22:403-411 (1988).

11. Böhnig, M., Feldermann, Chr. Jander, J., Lüers, B., Rudolph, G. and Wagner, H.Gg., *Proc. Combust. Inst.* 23:1581-1587 (1990).

12. Hanisch S., Jander, H., Pape, Th. and Wagner, H. Gg., *Proc. Combust. Inst.* 25:577-584 (1994).

13. Bauerle, St., Karasevich, Y., Slavov, St., Tanke, D., Tappe, M., Thienel, Th. and Wagner, H. Gg., *Proc. Combust. Inst.* 25:627-634 (1994).

14. Xu, F., Sunderland, P.B. and Faeth, G.M., *Combust. Flame* 108:471-493 (1997).

15. Xu, F., Lin, K.-C. and Faeth, G.M., *Combust. Flame* 115:195-209 (1998).

16. Xu, F. and Faeth, G.M., *Combust. Flame* 121:640-650 (2000).

17. Takahashi, F. and Glassman, I., *Combust. Sci. Tech.* 37:1-19 (1984).

18. Street, J.C. and Thomas, A., *Fuel* 34:4-36 (1955).

19. Flossdorf, J. and Wagner, H.Gg., *Z. Phys. Chem. Neue Folge* 54:113-120 (1967).

20. Calcote, H.F. and Miller, W.J., "Ionic Mechanisms of Carbon Formation in Flames," AeroChem Research Laboratories Paper No. TP-371, 1978.

21. Harris, M.M., Keng, G.B. and Laurendeau, N.M., *Combust. Flame* 64:99-112 (1986).

22. Markatou, P., Wang, H. and Frenklach, M., *Combust. Flame* 93:467-482 (1993).

23. Law, C.K., *Proc. Combust. Inst.* 22:1381-1402 (1988).

24. Kwon, S., Tseng, L.-K. and Faeth, G.M., *Combust. Flame* 90:230-246 (1992).

25. Tseng, L.-K., Ismail, M.A. and Faeth, G.M., *Combust. Flame* 95:410-426 (1993).

26. Aung, K.T., Tseng, L.-K., Ismail, M.A. and Faeth, G.M., *Combust. Flame* 102:526-530 (1995).

27. Hassan, M.I., Aung, K.T. and Faeth, G.M., *J. Prop. Power* 13:239-245 (1997)

28. Aung, K.T., Hassan, M.I. and Faeth, G.M., *Combust. Flame* 109:1-24 (1997).

29. Aung, K.T., Hassan, M.I. and Faeth, G.M., *Combust. Flame* 112:1-15 (1998).

30. Aung, K.T., Hassan, M.I. and Faeth, G.M., *Combust. Flame* 113:282-284 (1998).

31. Hassan, M.I., Aung, K.T., Kwon, O.C. and Faeth, G.M., *Combust. Flame* 115:539-550 (1998).

32. Hassan, M.I., Aung, K.T., Kwon, O.C. and Faeth, G.M., *J. Prop. Power* 14:479-488 (1998).

33. Kwon, O.C., Aung, K.T., Tseng, L.-K., Ismail, M.A. and Faeth, G.M., *Combust. Flame* 116:310-312 (1999).

34. Kwon, O.C., Hassan, M.I. and Faeth, G.M., *J. Prop. Power* 16:513-522 (2000).

35. Kwon, O.C. and Faeth, G.M., *Combust. Flame* 124:590-610 (2001).

36. Aung, K.T., Hassan, M.I., Kwon, S., Tseng, L.-K., Kwon, O.C. and Faeth, G.M., *Combust. Sci. Tech.* 174:1-40 (2001).

37. Kim, C.H., Kwon, O.C. and Faeth, G.M., *J. Prop. Power* 18:1059-1067 (2002).

38. Faeth, G.M., Kim, C.H. and Kwon, O.C., *Int. J. Environ. Combust. Tech.*, in press.

39. Strehlow, R.A. and Savage, L.D., *Combust. Flame* 31:209-211 (1978).

40. Sunderland, P.B., Mortazavi, S., Faeth, G.M. and Urban, D.L., *Combust. Flame* 96:97-103 (1994).

41. Urban, D.L., Yuan, Z.-G., Sunderland, P.B., Linteris, G.T., Voss, J.E., Lin, K.-C., Dai, Z., Sun, K. and Faeth, G.M., *AIAA J.* 36:1346-1360 (1998).

42. Xu, F. and Faeth, G.M., *Combust. Flame* 125:804-819 (2001).

43. Xu, F., El-Leathy, A.M., Kim, C.H. and Faeth, G.M., *Combust. Flame*, in press.

44. El-Leathy, A.M., Xu, F., Kim, C.H. and Faeth, G.M., *AIAA J.*, in press.

45. Koylu, U.O. and Faeth, G.M., *J. Heat Trans.* 115:409-417 (1993).

46. Charalampopoulos, T.T., *Prog. Energy Combust. Sci.* 18:13-45 (1992).

47. Faeth, G.M. and Koylu, U.O., *Combust. Sci. Tech.* 108:207-229 (1995).

48. Jullien, R. and Botet, R., *Aggregation and Fractal Aggregates*, World Scentific, Singapore, pp. 45-60 (1987).

49. Tien, C. L. and Lee, S. C., *Prog. Energy Combust. Sci.* 8:41-59 (1982).

50. Viskanta, R. and Mengüc, M.P., *Prog. Energy Combust. Sci.* 13:511-524 (1987).

51. Krishnan, S.S., Lin, K.C. and Faeth, G.M., *J. Heat Trans.* 122:517-524 (2000).

52. Wu, J.-S., Krishnan, S.S. and Faeth, G.M., *J. Heat Trans.* 119:230-237 (1997).

53. Koylu, U.O. and Faeth, G.M., *Combust. Flame* 89:140-156 (1992).

54. Dobbins, R.A., Mulholland, G.W. and Bryner, N.P., *Atmospheric Environment* 28:889-897 (1994).

55. Choi, M.Y., Mulholland, G.W., Hamins, A. and Kashiwagi, T., *Combust. Flame* 102:161-169 (1995)..

56. Mulholland, G.W. and Choi, M. Y., *Proc. Combust. Inst.* 27:1515-1522 (1998).

57. Zhou, Z.-Q., Ahmed, T.U. and Choi, M.Y., *Exp. Therm. Fluid Sci.* 18:27-32 (1998).

58. Dalzell, W.H. and Sarofim, A.F., *J. Heat Trans.* 91: 100-104 (1969).

59. Stagg, B.J. and Charalampoulos, T.T., *Combust. Flame* 94:381-396 (1993).

60. Dobbins, R.A. and Megaridis, C.M., *Appl. Optics* 30:4747-4754 (1991).

61. Koylu, U.O. and Faeth, G.M., *J. Heat Trans.* 111:409-417 (1993).

62. Chang, H.Y. and Charalampopoulos, T.T., *Proc. R. Soc. London A* 430:577-591 (1990).

63. Vaglieco, B.M., Beretta, F. and D'Alessio, A., *Combust. Flame* 79:259-271 (1990).

64. Krishnan, S.S., Lin, K.C. and Faeth, G.M., *J. Heat Trans.* 123:331-339 (2001).

65. Koylu, U.O. and Faeth, G.M., *J. Heat Trans.* 116:152-159 (1994).

66. Koylu, U.O. and Faeth, G.M., *J. Heat Trans.* 118:415-421 (1996).

67. Koylu, U.O., Faeth, G.M., Farias, T.L. and Carvalho, M.G., *Combust. Flame* 100:621-633 (1995).

68. Manickavasagam, S. and Mengüc, M.P., *Energy and Fuel* 7:860-869 (1993).

69. Koylu, U.O. and Faeth, G.M., *J. Heat Trans.* 116:971-979 (1994).

70. Rudder, R.R. and Bach, D. R., *J. Opt. Soc. Amer.* 58:1260-1266 (1968).

71. Farias, T.L., Koylu, U.O. and Carvalho, M.C., *Appl. Optics* 35:6560-6567 (1996).

72. Bohren, C.F. and Huffman, D.R., *Absorption and Scattering of Light by Small Particles*, Wiley, New York, 1983, pp. 477-482.

73. diStasio, S., *Appl. Phys.* B70:635-643 (2000).

74. Felske, J.D., Charalampopoulos, T.T. and Hura, H., *Combust. Sci. Tech.* 37:263-284 (1984).

75. Batten, C.E. Appl. Opt. 24:1193-1199 (1985).

76. Lee, S.C. and Tien, C.L., *Proc. Combust. Inst.* 18:1159-1166 (1980).